Efficient Collaborative (Viral) Communication in OFDM Based WLANs

Aggelos Bletsas and Andrew Lippman

Media Laboratory
Massachusetts Institute of Technology
20 Ames St, E15-495, Cambridge, MA 02139, USA
{aggelos,lip}@media.mit.edu

Abstract

In this work we investigate the coordinated transmission and processing of distributed radios employing OFDM signals similar to those employed in 802.11a. After showing that OFDM can be viewed as a set of parallel Gaussian channels with different frequency gain for each subcarrier, we design receiving schemes that exploit both the direct transmission between transmitter and receiver as well as the assisting relayed signal of a radio that overhears the communication between transmitter and receiver and acts as an analogue repeater. The special structure of 802.11a OFDM signals allow the coordination between transmitter, receiver and intermediate relay to happen on the same channels and the collaboration results in substantial energy savings compared to the traditional single transmitter-single receiver case, providing efficient resource (energy, bandwidth) utilization.

1 Introduction

Decentralized wireless communications has been in the scientific spotlight for several decades. Recent information theoretic papers have shown that cooperative communication between network nodes can increase the overall transport capacity of the network [2]. Therefore, there is a strong interest for practical algorithms and schemes for collaborative wireless communication.

Inspired by [3], [4] where diversity techniques were exploited over two channels, one for the direct transmission between transmitter and receiver and one for the relayed transmission from an intermediate relay node, we propose a *single channel* collaborative communication scheme, exploiting the special properties of OFDM signals, in 802.11a based WLANs.

We call these communications systems viral because they use opportunistic cooperation among the nodes, exploiting any intermediate ones to propagate the messages. The *viral* communication scheme proposed achieves significant energy savings compared with the direct, non-collaborative case. Since the collaboration happens within the same channels as the direct case, we have an improvement that directly leads to more efficient resource utilization (energy, bandwidth) in a network sense, that potentially can lead to better scalability and therefore higher overall network capacity.

In section 2 we present the properties of the OFDM signals, necessary for our viral scheme, in section 3 we provide the details of the transmitters and receivers as well as theoretical performance bounds and finally in section 4 we provide the experimental results. We conclude in section 5 with some comments on how this system can be used.

2 OFDM Properties and Viral Communication

In this section we are going to explain the suitability of Orthogonal Frequency Division Multiplexing (OFDM) signals for collaborative communication in ways we nominate them as "viral" and present in the rest of this paper.

$$x(t) = \frac{1}{N}\sum_{-k}^{k}(X_k e^{+j2k\pi\Delta f t}) \quad (1)$$

The baseband OFDM signal (in equation 1) is the sum of $N \geq 2k+1$ orthogonal carriers modulating N information symbols. For 802.11a N is 64 even though 48 carriers are used for data, 4 are used for frequency synchronization and the rest are zeroed obtaining spacing in the frequency domain [5]. The symbols X_k are set according to BPSK, QPSK or QAM modulation schemes and generally are complex numbers [5]. The orthogonality between the sub-carriers is ensured by setting the spacing between them equal to the OFDM signal $x(t)$ duration T :

$$T = \frac{1}{\Delta f} \quad (2)$$

Sampling this baseband signal $x(t)$ and acquiring $N = T/\delta t$ samples leads to the familiar IDFT formula (4), which implies that the baseband signal could be constructed

by passing the $N\{x_n\}$ samples over fast IFFT modules and then through efficient analogue-to-digital converters (ADCs).

$$x_n = x(n\delta t) = \frac{1}{N}\sum_{-k}^{k}(X_k e^{+j2k\pi n/N}) \quad (3)$$

$$\Rightarrow x_n = IDFT\{X_k\} \quad (4)$$

It is interesting to see that oversampling this ideally constructed OFDM baseband signal with double frequency ($\delta t' = \delta t/2$) and consequently observing $x(t)$ at half of its duration T ($N\delta t' = N\delta t/2 = T/2$), can still lead to the observation of the original N information symbols X_k :

$x(n\delta t') = x(n\delta t/2) = \frac{1}{N}\sum_{-k}^{k}(X_k e^{+j2k\pi\Delta f\ n\ \delta t/2})$

$= \frac{1}{N}\sum_{-k}^{k}(X_k\ e^{+j2k\pi n/2N})$

$= \frac{1}{N}\sum_{-k}^{k}(X_k\ e^{+j2k\pi n/2N}\ e^{+j2k\pi n/2N}\ e^{-j2k\pi n/2N})$

$= \frac{1}{N}\sum_{-k}^{k}\{(X_k\ e^{-jk\pi n/N})\ e^{+j2k\pi n/N}\}$

$\Rightarrow x'_n = x(n\delta t') = IDFT\{X_k\ e^{-jk\pi n/N}\}$

From the last relationship we can see that observing the baseband signal $x(t)$ at half duration, *by means of oversampling*, results in a phase shift of the original information symbols by a known factor for every symbol X_k. Therefore, provided that we have an ideally constructed OFDM symbol $x(t)$ the following first property occurs:

- **Property 1**: Observation of an OFDM signal at half its duration could provide for the estimation of the information symbols X_k.

Another important characteristic of the 802.11a signal structure is the cyclic prefix added to each signal $x(t)$. That prefix is derived from the last 1/4 part of $x(t)$ and its duration of 0.8 μs ($x(t)$ duration T=3.2 μs) is larger than the maximum delay spread of the wireless channel (for the transmission power levels and reception ranges specified in the protocol [5]) ensuring zero inter-symbol interference (ISI) regardless the location between transmitter and receiver. That means that node 1 and 2 simultaneous transmissions in figure 1 could coincide at node 3 since the difference in the propagation times is absorbed by the cyclic prefix of the transmitted signals. Therefore the second important property occurs:

- **Property 2**: Simultaneous transmissions in 802.11a networks could lead to simultaneous receptions with zero ISI regardless the topology of the network.

The above properties enable the *Viral* wireless communication scheme presented in the following section. Before proceeding, it is useful to see that OFDM can be viewed as a set of N parallel channels (one for each sub-carrier), with different channel gains for each sub-carrier:

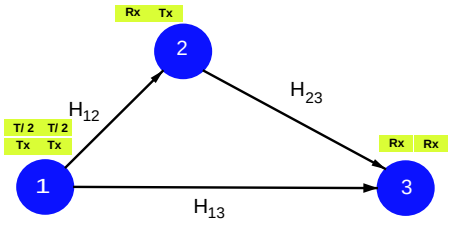

Figure 1: The simple topology examined in this work. Node 1 transmits, Node 3 receives and Node 2 receives during the first half of the signal duration and re-transmits during the second half of the signal duration.

Theorem 2.1 *The convolution of a baseband OFDM signal $x(t)$ with the wireless channel impulse response $\sum_{m=0}^{L-1}(h_m\,\delta(t-\tau_m))$ results in a new baseband signal $r(t) = x(t) * h(t)$ with information symbols $\{H(k)\ X_k\}$, where $\{H(k)\} = DFT\{h_m\} = DFT\{h_0, h_1, \cdots, h_{L-1}, \underbrace{0, 0, \cdots, 0}_{N-L}\}$.*

The proof is provided at the Appendix.

The analysis is simplified since the convolution with the channel multiplies each information symbol X_k with a complex number $H(k)$ that represents the channel frequency response at the corresponding sub-carrier.

3 Viral Communication

3.1 System Model

In the previous section it was shown that observation of the OFDM signal at half of its duration (through oversampling) results in a known phase shift of the information signals $\{X_k\}$. It was also shown that the wireless channel filters the OFDM signal by a multiplication of the information symbols $\{X_k\}$ with a frequency response per sub-carrier $H(k)$.

Having in mind the above, we devised a simple scheme for collaborative communication, part of a greater theme of collaborative radio communication: node 1 transmits an OFDM signal $s(t)$ (figure 1) to node 3. The intermediate node 2 "observes" the signal for the first half $T/2$ of its duration (through oversampling), amplifies it (amplifying also its own noise) and retransmits during the second half of the signal duration $s(t)$. Node 3 also over-samples and receives during the first half the direct transmission of $s(t)$ while during the second half, node 3 receives the direct (from node 1) as well as the relayed transmission (from node 2).

For each information symbol X_k (out of the N in the baseband signal $x(t)$) it can be analytically derived (the derivation has been omitted due to space restrictions) that node 3 during the first half of signal duration receives v_{31}:

$$v_{31} = H_{13}X_k + z_{31} \quad (5)$$

and during the second half of signal duration node 3 receives v_{32}:

$$v_{32} = H_{13}X_k + \beta H_{23}\hat{X}_k + z_{32} \quad (6)$$

where the phase shift of $\{X_k\}$ due to oversampling has been incorporated in the channel coefficients H_{ij} which are modeled as iid, complex zero-mean Gaussian random variables with variance $\sigma_{ij}^2/2$ per dimension. Each variance σ_{ij}^2 could be further modeled as $\sigma_{ij}^2 = \frac{G}{d_{ij}^v}$ where G represents the antenna gains of the nodes i and j, d_{ij}^v is the distance between i and j and v is the propagation coefficient of the medium, with $2 \leq v \leq 4$ [7]. The variables z_2, z_{31} and z_{32} represent internal noise of the receiver 2, 3 (first half) and 3 (second half) and can be modeled as iid, complex zero-mean Gaussian random variables with variance $N_0/2$ per dimension. Under those assumptions the magnitude $|H_{ij}|$ of the channel coefficients is distributed according to a Rayleigh distribution and the square magnitude according to an exponential distribution with $E[\,|H_{ij}|^2\,] = \sigma_{ij}^2$.

We assume quasi-static fading model where the channel coefficients H_{ij} remain constant through several consecutive transmissions of the OFDM signals, an assumption which is valid since the symbol duration is on the order of μsecs while the channel tends to change within msecs [7]. It is also important to note that the channel coefficients are computed using special known training sequences. The above model is a baseband model, therefore we have omitted the challenging tasks of frequency and timing offset estimation, in a network sense [1], between nodes 1, 2 and 3. Future protocols for collaborative radio communication should incorporate network channel estimation and network time and frequency synchronization (as opposed to point-to-point estimation techniques currently practiced).

Equations 5, 6 refer to the first and second half of the signal $s(t)$ transmitted from node 1 (figure 1), therefore the collaboration between nodes 2 and 3 is happening within the same signal duration (*the same channel*), as opposed to the non-OFDM schemes proposed in [3]. That is possible only because of the properties of OFDM explained in section 2.

In equation 6, $\hat{X}_k$ represents the signal that node 2 is relaying (figure 1). As described in [3], there are two options: either decode using standard estimation techniques (like a ML receiver) and regenerate or just amplify and forward (act as an analogue repeater). The second technique was more efficient as we experimentally verified and that was the technique followed in this work:

$$\hat{X}_k = \beta(H_{12}X_k + z_2) \quad (7)$$

$$\text{eq. } (5), (6), (7) \Rightarrow$$

$$v_{31} = H_{13}X_k + z_{31} \quad (8)$$

$$v_{32} = (H_{13} + \beta H_{12}H_{23})X_k + \beta H_{23}\, z_2 + z_{32} \quad (9)$$

As we have said, the information symbol X_k is generally a complex number which is set according to the modulation scheme practiced (BPSK, QPSK, QAM). We will compare the above collaborative scheme with the non-collaborative point-to-point case, using BPSK. We will denote as E the energy per bit used in the point-to-point case, $E1$ the energy per bit used at the transmission of node 1 and $E2$ at node 2 in the viral (collaborative) scheme.

For BPSK, $X_k = \pm\sqrt{E}$ in the non-collaborative case and more particularly:

$$'0' : v = +H_{13}\sqrt{E} + z_3 \quad (10)$$

$$'1' : v = -H_{13}\sqrt{E} + z_3 \quad (11)$$

and the ML receiver for equi-probable bits is the following:

$$Re\{v\, H_{13}^*\sqrt{E}\} \lessgtr_{'0'}^{'1'} 0 \quad (12)$$

The probability of error for this receiver, given knowledge of H_{13} ($\gamma_{13} = |H_{13}|^2 E/N_0$) is

$$P_{e/H_{13}} = Q\left(\sqrt{\frac{|H_{13}|^2 E}{N_0/2}}\right) = Q(\sqrt{2\gamma_{13}}) \quad (13)$$

where $Q(x) = \frac{1}{\sqrt{2\pi}}\int_x^{+\infty} e^{-x^2/2}$. Integrating the above relationship over the exponential distribution of γ_{13} we obtain the following probability of error [6]:

$$P_e = \frac{1}{2}\left(1 - \sqrt{\frac{\bar{\gamma_{13}}}{1+\bar{\gamma_{13}}}}\right) \simeq \frac{1}{4\,\bar{\gamma_{13}}} \qquad \bar{\gamma_{13}} \gg 1 \quad (14)$$

where $\bar{\gamma_{13}} = \sigma_{13}^2 E/N_0$ and σ_{13}^2 as defined above.

The last equation (equation (14)) will be used for the comparison of the direct, non-collaborative scheme with the collaborative (viral) one. Before proceeding to the performance results, we need to layout specific details about the viral transmitter and receiver.

3.2 Viral Transmission

In section 2 we showed that oversampling of an ideally constructed OFDM signal $s(t)$ results in a known phase shift ($e^{+jk\pi n/N}$) of the information symbols $\{X_k\}$. Since the intermediate node 2 (figure 1) over-samples during the first half signal duration and destination node 3 over-samples during the first and second half of the signal duration, the signal to be transmitted should be an ideally constructed OFDM signal exhibiting the above property after oversampling.

Therefore, the transmitted signal during the first half should be constructed using the N modified symbols $\{X_k e^{+jk\pi n/N}\}$ through an IDFT procedure. The same process should be followed during the second half of the signal duration at node 1 as well as during the transmission of the intermediate node 2. With that simple modification (since that involves a simple phase shift in software) "ideal" OFDM signals for viral communication are constructed.

3.3 Viral Reception

From equation (7) it is easy to see the relationship between the amplification β of the relayed symbol X_k with the transmission energies E1, E2 at node 1 and 2 respectively:

$$\text{eq. (7)} \Rightarrow \beta^2 |H_{12}|^2 E1 + \beta^2 N_0 = E2 \quad \Rightarrow$$
$$\beta^2 = \frac{E2}{|H_{12}|^2 E1 + N_0} \tag{15}$$

For the simple BPSK system presented below z_1, z_2 are iid complex, zero-mean Gaussian random variables with variance $\frac{N1}{2}$, $\frac{N2}{2}$ per dimension respectively and H_1, H_2 are known, iid complex coefficients, according to a Gaussian distribution:

$$y_1 = H_1 X + z_1 \tag{16}$$
$$y_2 = H_2 X + z_2 \tag{17}$$
$$'0' : X = +\sqrt{E}$$
$$'1' : X = -\sqrt{E}$$

the (optimum) ML receiver is the following *Maximum Ratio Combining* receiver, which is simply a straightforward consequence of detection of vector observations:

$$\frac{4\sqrt{E}}{N_1} Re\{y_1 H_1^*\} + \frac{4\sqrt{E}}{N_2} Re\{y_2 H_2^*\} \lessgtr_{'0'}^{'1'} 0 \tag{18}$$

The probability of error for this ML receiver, given knowledge of H_1, H_2 is:

$$P_{e/H_1,H_2} = Q\left(\sqrt{\frac{2|H_1|^2 E}{N_1} + \frac{2|H_2|^2 E}{N_2}}\right) \tag{19}$$

Integrating the above probability of error over the exponential distribution of $|H_1|^2$, $|H_2|^2$ and using the inequality $Q(x) \leq \frac{1}{2} e^{-x^2/2}$ we have the following upper bound on the unconditional probability of error for the ML receiver above:

$$P_e \leq \frac{1}{2} \frac{1}{\frac{\overline{|H_1|^2} E}{N_1} + 1} \frac{1}{\frac{\overline{|H_2|^2} E}{N_2} + 1} \tag{20}$$

We apply the above results in our system model described in equations 8, 9 having in mind that for BPSK $X_k = +\sqrt{E1}$ for '0' and $X_k = -\sqrt{E1}$ for '1'. The Maximum Ratio Combining receiver is the following:

$$Re\{\frac{\sqrt{E1}\, v_{31}\, H_{13}^*}{N_0}\} +$$
$$+ Re\{\frac{\sqrt{E1}\, v_{32}\, (H_{13}^* + b\, H_{12}^* H_{23}^*)}{b^2 |H_{23}|^2 N_0 + N_0}\} \lessgtr_{'0'}^{'1'} 0 \tag{21}$$

Based on equation 20 and the system model equations 8, 9, we provide the following upper bound on the unconditional error probability of our receiver, which was experimentally proved a tight bound for locations of the intermediate node 2 alongside the line between transmitter 1 and receiver 3:

$$P_e \leq \frac{1}{2} \frac{1}{(\overline{\gamma_{13}} + 1) \frac{\overline{\gamma_{13}} + \frac{\overline{\gamma_{12}}\,\overline{\gamma_{23}}}{\overline{\gamma_{12}} + N_0}}{N_0 + \frac{\overline{\gamma_{23}} N_0}{N_0 + \overline{\gamma_{12}}}}} \tag{22}$$

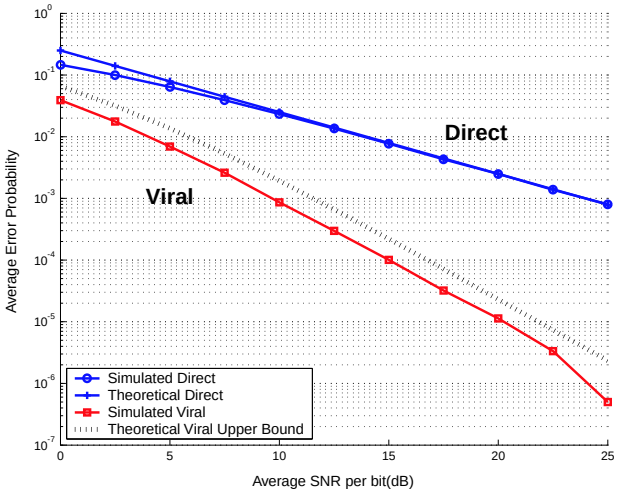

Figure 2: Error Probability for E1=E2=E/2, $d_{12} = d_{23} = 0.5$, $d_{13} = 1$ and v=4.

where $\overline{\gamma_{ij}} = \sigma_{ij}^2 Ei/N_0$ and $\sigma_{ij}^2 = \overline{|H_{ij}|^2} \simeq \frac{G}{d_{ij}^v}$ as defined above.

We are ready now to proceed to the experimental results.

4 Performance

After normalizing the distance between nodes 1 and 3 to $d_{13} = 1$ we evaluated our *single channel* viral receiver (equation 21) according to the system model (equations 8, 9) and compared with the direct point-to-point transmission (equations 10, 11). Initially, we kept the total transmission energy E1+E2 of the viral scheme equal to the transmission energy E of the direct, single hop case and we plotted the error probability after the simulations as well as the theoretical upper bounds calculated from the equations 14, 22 for the direct and viral case respectively, versus the average single hop SNR per bit $\frac{E}{N_0}\sigma_{13}^2$ where $\sigma_{ij}^2 \simeq \frac{G}{d_{ij}^v}$.

In figure 2 where the intermediate node is half way between transmitter and receiver, the probability of error is one to three orders of magnitude smaller than that of the direct case, for the same energy used. Similar remarkable behavior is observed in figures 3, 4 where the intermediate node is either closer to the transmitter or closer to the receiver. Similar behavior was observed in the experiments in [3] where two channels were used, one for the direct transmission and one for the relay.

It is interesting to quantitatively find out the energy gains due to collaboration using the above single channel viral scheme. Using equations 14 and 22 which describe the error probability for the direct and the viral scheme respectively, we performed the minimization of energies E and (E1, E2) given a specific target error probability and plotted the computed ratio $\frac{E}{E1+E2}$. From figures 5, 6 we can also see an approximately two orders of magnitude energy saving for an

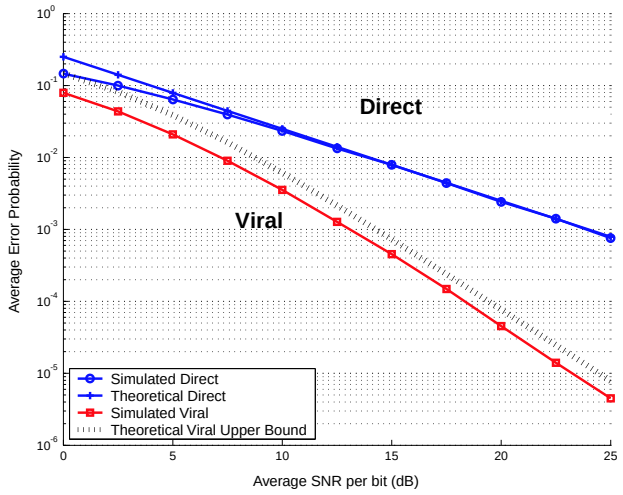

Figure 3: Error Probability for E1=E2=E/2, $d_{12} = 0.1$, $d_{23} = 0.9$, $d_{13} = 1$ and v=4.

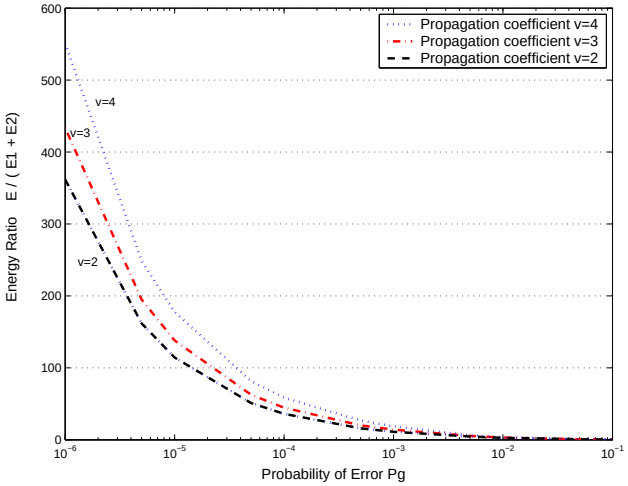

Figure 5: Energy ratio between the energy used in direct transmission E and energy used in viral scheme E1+E2 versus target error probability with $d_{12} = d_{23} = 0.5$ and $d_{13} = 1$.

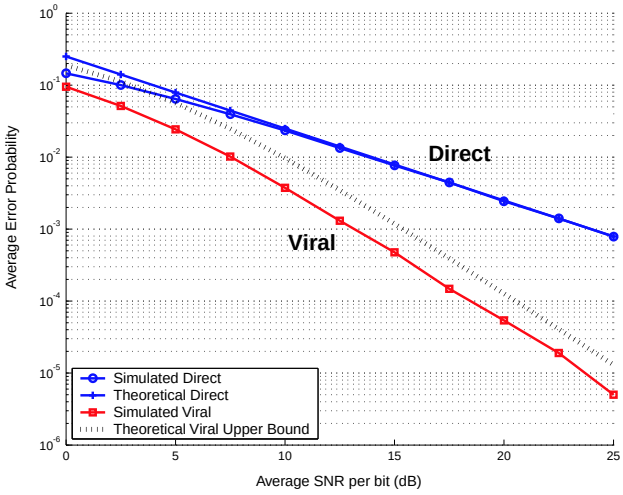

Figure 4: Error Probability for E1=E2=E/2, $d_{12} = 0.9$, $d_{23} = 0.1$, $d_{13} = 1$ and v=4.

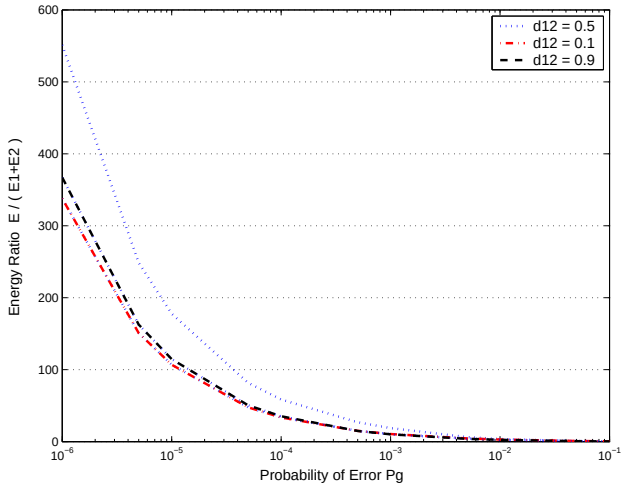

Figure 6: Energy ratio between the energy used in direct transmission E and energy used in viral scheme E1+E2 versus target error probability with $d_{13} = 1$, v=4.

intermediate relay across the connecting line between transmitter and receiver, for all tested values of the propagation coefficient v. Savings with this viral scheme were also observed for a relay in the vicinity of transmitter and receiver, however precise topology bounds were not possible to derive due to the complexity of equation 22 (and its inaccuracy at regions away from the area between transmitter and receiver). We will address the problem of suitable topologies for viral communication in future work.

5 Conclusion

In the above sections we demonstrated a "viral" scheme for single channel, collaborative, wireless communication. The collaboration resulted in energy savings or in higher reliability (smaller error probability) for the same energy used, compared with the direct, non-collaborative case. Since the collaboration happens within the same channels as the direct case, we have an improvement that directly leads to more efficient resource utilization (energy, bandwidth) in a network sense, that potentially can lead to better scalability and therefore higher overall network capacity.

In addition to the ability of such a system to scale through the re-use of the channel in the same region, this system propagates the message through relay nodes with a delay that is small compared to the information rate. Thus, it can be used for realtime applications such as telephony. The essence of the plan is that the information is passed from node to node without decoding and remodulating the messages.

Nevertheless, there are important technical challenges to be explicitly addressed like network frequency/phase/time synchronization and distributed channel estimation as well as important sociological issues like privacy/security and economics to be discussed. We have just scratched the surface and exciting research horizons are now opened.

References

[1] A. Bletsas. *"Evaluation of Kalman Filtering for Network Time Keeping"*. IEEE Pervasive Computing and Communication Conference (Percom 2003), March 2003.

[2] P. Gupta and P. R. Kumar. *"The Capacity of Wireless Networks"*. IEEE Transactions on Information Theory, March 2000.

[3] J. N. Laneman and G. W. Wornell. *"Energy-Efficient Antenna-Sharing and Relaying for Wireless Networks"*. Proc. IEEE Wireless Communications and Networking Conference (WCNC-2000), September 2000.

[4] J. N. Laneman and G. W. Wornell. *"Distributed Spatial Diversity Techniques for Improving Mobile Ad-Hoc Network Performance"*. Proc. of ARL FedLab Symposium on Advanced Telecommunications and Information Distribution (ATIRP-2001), March 2001.

[5] IEEE Standard for Information Technology. *Part 11: Wireless LAN Medium Access Control (MAC) and Physical Layer (PHY) Specification (802.11a)*. 1999.

[6] J. G. Proakis. *Digital Communications*. McGraw-Hill, 4th edition, 2001.

[7] T. S. Rappaport. *Wireless Communications: Principles and Practice*. Prentice-Hall, 2th edition, 2002.

APPENDIX

Theorem: *The convolution of a baseband OFDM signal $x(t)$ with the wireless channel $\sum_{m=0}^{L-1}(h_m\,\delta(t-\tau_m))$ results in a new baseband signal $r(t) = x(t) * h(t)$ with information symbols $\{H(k)\ \ X_k\}$, where $\{H(k)\} = DFT\{h_m\} = DFT\{h_0, h_1, \cdots, h_{L-1}, \underbrace{0, 0, \cdots, 0}_{N-L}\}$.*

Proof :

$r(t) = x(t) * h(t) =$

$= \frac{1}{N}\sum_{k=-K}^{K}\sum_{m=0}^{L-1} h_m X_k e^{+j2\pi k(t-t_m)/T}$

$= \frac{1}{N}\sum_k X_k e^{+j2\pi kt/T}\sum_m h_m e^{+j2\pi kt_m/T}$

$\simeq \frac{1}{N}\sum_k X_k e^{+j2\pi kt/(N\delta t)}\sum_m h_m e^{+j2\pi km\delta t/(N\delta t)}$

$= \frac{1}{N}\sum_k X_k e^{+j2\pi kt/(N\delta t)}\underbrace{\sum_m h_m e^{+j2\pi km/N}}_{DFT\{h_m\}=H(k)}$

$= \frac{1}{N}\sum_k H(k)X_k e^{+j2\pi kt/(N\delta t)} \Rightarrow$

$r(n\delta t) = \frac{1}{N}\sum_k H(k)X_k e^{+j2\pi kn/N} =$

$= IDFT\{H(k)X_k\} \quad \mathbf{Q.E.D.}\ \square$